Organic & Biomolecular Chemistry

Cite this: *Org. Biomol. Chem.*, 2011, **9**, 5109

www.rsc.org/obc

PAPER

A significant role of alkaline cations on the Reimer–Tiemann reaction†

Shinichi Yamabe and Takeshi Fukuda

Received 15th March 2011, Accepted 20th April 2011
DOI: 10.1039/c1ob05405h

The Reimer–Tiemann (R–T) reaction was investigated by DFT calculations. A model composed of $CHCl_3$, $PhO^-(Na^+)H_2O$ and $[NaOH(H_2O)_2]_2$ was employed for geometry optimizations. A K^+-containing model was also investigated. The dichlorocarbene reagent, which has been thought of for a long time, was found to intervene only transiently in the carbenoid form. In this form, the Na^+ (or K^+) coordination to CCl_2 enhances its electrophilicity toward $C_6H_5O^-$. The counter ion also works to stabilize the precursor phenoxide ion and intermediates of the substituted phenoxides in the hexagonal pyramidal coordination. The Na^+-containing reaction consists of seven elementary processes, (K^+, six ones) with extremely high exothermicity and spontaneity.

I. Introduction

The Reimer–Tiemann (herein, R–T) reaction is used for the *ortho*-formylation of phenols. The reaction was discovered by Karl Ludwig Reimer and Ferdinand Tiemann in 1876.[1] In the typical case, the product is salicylaldehyde in Scheme 1.

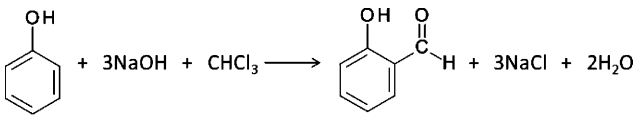

Scheme 1 A representative Reimer–Tiemann (R–T) reaction.

As a reagent, chloroform serves as a source of the dichlorocarbene CCl_2.[2] That is, $CHCl_3$ reacts with aqueous sodium hydroxide to produce CCl_2.[3–6] The production is shown as the first line of Scheme 2. This reagent effects *ortho*-formylation of activated aromatic rings in the phenoxide ion $C_6H_5O^-$ in the second line of Scheme 2. After basic hydrolysis of the dichloromethyl-substituted phenol, the aldehyde product is formed in the third line of Scheme 2.

The mechanism of Scheme 2 appears to be well-established nowadays. However, there remain some questions. Firstly, the reactant chloroform and the product salicylaldehyde have one C–H covalent bond. Therefore, a C–H bond-retaining reaction appears to be likely, which is different from the processes in Scheme 2. That is, is the direct *ortho*-formylation of phenols really unlikely as suggested?[7] Secondly, the driving force of carbene CCl_2 formation is unknown. Thirdly, the carbene is very unstable, and it is questionable whether it can intervene in the aqueous solvent. Water molecules are very nucleophilic when they are bound in the cluster form.[8] Fourthly, are counter ions Na^+ and K^+ concerned with the reaction's progress?

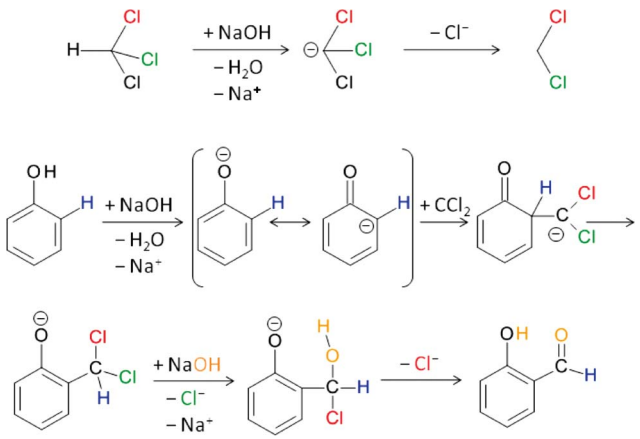

Scheme 2 A scheme of the R–T reaction containing the dichlorocarbene CCl_2.

In spite of the classic reaction, there have been no theoretical studies of phenol formylation. Only a computational study of the R–T reaction between the conjugate anion of pyrrole and dichlorocarbene with one water molecule has been reported.[9] From the carbene adduct (I1N), the intramolecular H[1,2] hydrogen shift transition state (TS) was shown to be the rate-limiting step. However, an intermolecular hydrogen shift would be more likely than an intramolecular one, which has a three-membered ring strain TS geometry. In this work, B3LYP calculations were carried out to investigate the mechanism of the R–T reaction in consideration of the above four questions.

II. Method of calculations

Geometries were determined by density functional theory calculations at the RB3LYP/6-31(+)G(d) level,[10] where the diffuse orbital

Department of Chemistry, Nara University of Education, Takabatake-cho, Nara-shi, 630-8528, Japan. E-mail: yamabes@nara-edu.ac.jp

† Electronic supplementary information (ESI) available. See DOI: 10.1039/c1ob05405h

"(+)" is added to the oxygen 6-31G(d) basis set.[11] This basis set was used because the size of the reacting system employed in the study is large (stoichiometry, $C_7H_{18}Cl_3Na_3O_8$ or $C_7H_{18}Cl_3K_3O_8$). For the Na^+-containing system, RB3LYP/6-31+G* geometry optimizations were also carried out.

TSs were characterized by vibrational analysis, by which we examined whether the Hessian matrices obtained from TS geometries had single imaginary frequencies ($\upsilon^{\ddagger}$). From the TSs, reaction paths were followed using the IRC (intrinsic reaction coordinate) method[12] to obtain the minimum energy geometries. Relative free energies were calculated by the sum of the RB3LYP/6-31(+)G(d) [and RB3LYP/6-31+G(d)] thermal correction of the Gibbs free energy and the single-point energy of RB3LYP/6-311+G(d,p) SCRF═(PCM, solvent = water).[13]

For the Na^+ containing system, two TSs (TS1 and TS2) have similar high energies, and these were re-evaluated by six additional calculations, (a–f), to specify the rate-determining step.

(a) B3LYP/6-311+G(d,p) SCRF═PCM // B3LYP/6-311+G(d,p)

(b) MPW1K/6-311+G(d,p) SCRF═PCM // MPW1K/6-31(+)G(d)

(c) B3LYP/6-311++G(2d,p) SCRF═PCM // B3LYP/6-31(+)G(d)

(d) B3LYP/6-311++G(3df,2p) SCRF═PCM // B3LYP/6-31(+)G(d)

(e) B3PW91/6-311++G(3df,2p) SCRF═PCM // B3LYP/6-31(+)G(d)

(f) B3LYP/Aug-cc-pVDZ SCRF═PCM // B3LYP/6-31(+)G(d)

The DFT methods MPW1K[14] and B3PW91[15] are known to give interaction and activation energies reliably [*e.g.*, ref. 14*c* and 15*c*].

All calculations were carried out using the GAUSSIAN 03[16] program package installed at the Research Center for Computational Science, Okazaki, Japan.

III. Results and discussion

III-1 Origin of CCl_2 formation

The first examination was the presence or absence of the dichlorocarbene added into the water cluster. A geometry optimization of $CCl_2(H_2O)_{14}$ was carried out. The resultant geometry was found to be composed of carbon monoxide (CO), $(H_3O^+)_2$, $(Cl^-)_2$ and $(H_2O)_{11}$, as Fig. S1 in the ESI shows.† Indeed, the CO formation reported[4] was confirmed, but the carbene alone was computed to be absent from the water cluster. Since the solvent H_2O cannot support the appearance of CCl_2, the counter cation Na^+ might be contributive to it. Scheme 3a shows three geometric isomers of $Cl_3C^- \cdots Na^+$, i, ii and iii.

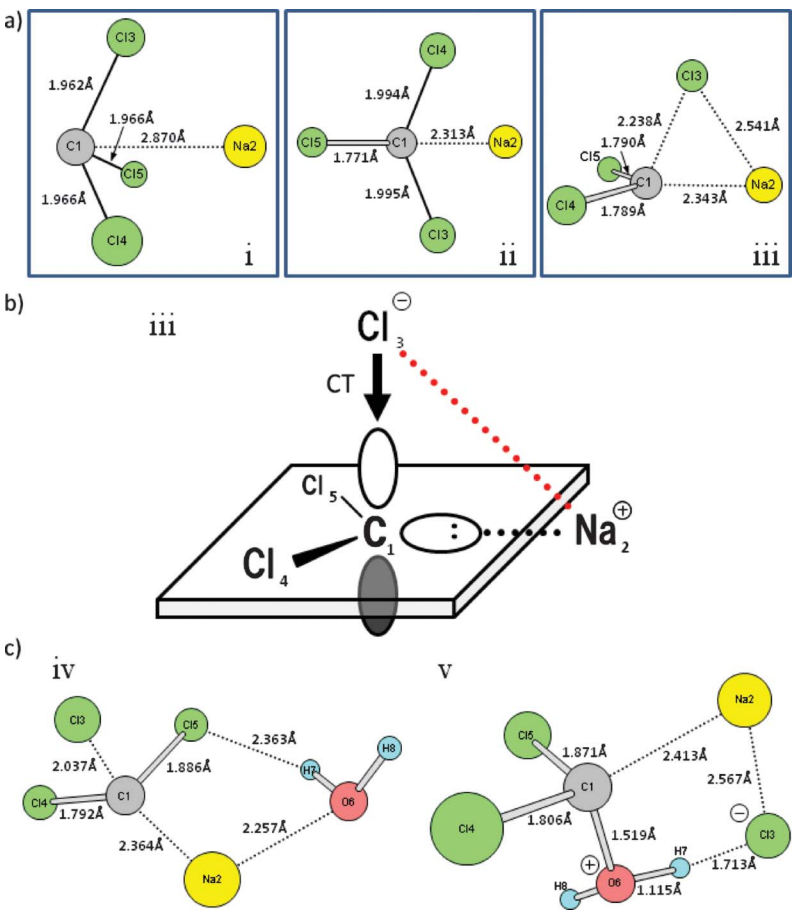

Scheme 3 (a) Three geometric isomers, i, ii and iii, of the Cl_3^-–Na^+ complex. (b) The orbital interaction for the carbenoid structure of isomer iii. CT is the charge transfer interaction. (c) Two geometric isomers, iv and v, of iii + H_2O. *i.e.* (Cl_3CNa + H_2O).

Among the three, isomer iii was found to consist of $Cl_2C\cdots Cl^-\cdots Na^+$. The triangle moiety in iii may be described by the interaction of Scheme 3b. The Na^+ ion is coordinated to the carbon lone-pair orbital along with the $Cl(3)^-\cdots Na(2)$ attraction. The electronic charge of chloride ion $Cl(3)^-$ is transferred to the axial vacant orbital of the carbene. The interacting system is a carbenoid. While the carbenoid is well known in the Simmons–Smith reaction[17] of Scheme 4, it has not been considered in the R–T reaction. The coordination strength of Na^+ has probably been thought to be much weaker than the transition metals used in the Simmons–Smith reaction.

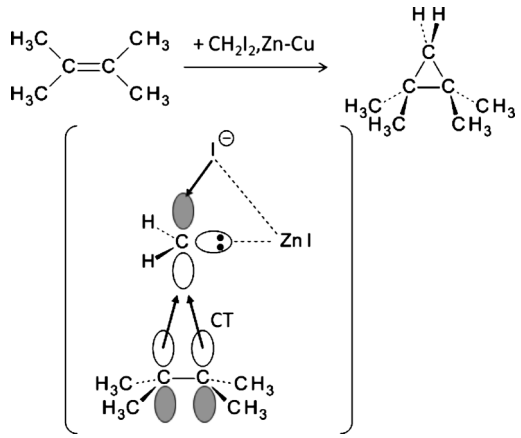

Scheme 4 A typical Simmons–Smith reaction (ref. 17) involving a carbenoid intermediate.

The first step of the R–T reaction, *i.e.*, electrophilic addition (CCl_2 to the phenoxide ion), then needs to be investigated by the use of carbenoid iii. When a base approaches the black lobe of the vacant orbital in Scheme 3b, chloride ion $Cl(3)^-$ leaves sensitively, as isomer v of ($Cl_3CNa + H_2O$) in Scheme 3c shows.

III-2 Search for the path of the R–T reaction

Scheme 5 shows the model employed in this study. It is composed of the $CHCl_3$ molecule, two sets of $NaOH(H_2O)_2$ and a phenoxide ion$(Na^+)H_2O$. One HO^- ion in $NaOH(H_2O)_2$ is used to convert $CHCl_3$ to CCl_3^-, and the other for the formation of the aldehyde group in the product.

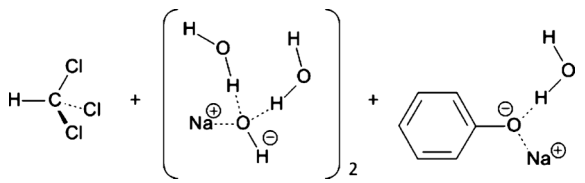

Scheme 5 The reaction model employed in the present calculations.

Fig. 1 shows TS geometries along the path. The other ones (*e.g.*, precursor(Na^+) and Int1(Na^+)) are exhibited in Fig. S2 of the ESI.† In the precursor, one Na^+ ion, Na(39), is coordinated to the phenyl π electronic cloud in a hexagonal pyramidal geometry. The binding energy (ΔE) of $PhO^-\cdots Na^+$ in the coordination was calculated to be 118.52 kcal mol^{-1} by B3LYP/6-311+G(d,p) // B3LYP/6-31(+)G(d), as shown in Fig. S3 of the ESI.† In TS1(Na^+), proton H(17) of Cl_3C–H is removed by the H(19)–O(18)$^-$ ion. After TS1(Na^+), the first intermediate, Int1(Na^+), is formed. In Int1(Na^+), the $CCl_3^-Na(39)^+$ species is involved. When this species moves onto the phenyl ring, Int2(Na^+) is formed. In Int2(Na^+), the carbenoid fragment $Na(39)\cdots C(9)Cl_2$ is involved, where the third Cl, Cl(16), is already far away from the CCl_2 moiety. This separation comes from charge transfer from *ortho* carbon C(4) of the phenoxide ion to the out-of-plane vacant orbital of the carbene. This separation is also shown on the right of Scheme 3c. Int2(Na^+) is very unstable and transient. Electrophilic addition of the carbenoid takes place at TS2(Na^+). The adduct is Int3(Na^+), which is followed by the proton H(22) attached to C(9) at TS3(Na^+). A neutral and novel dienone intermediate, Int4(Na^+), is generated. Next, by deprotonation of *ortho* hydrogen H(10) at TS4(Na^+), a substituted phenoxide ion $[C_6H_4(CHCl_2)–O^-]$ is recovered at Int5(Na^+). At the same time, the hexagonal pyramidal coordination of $Na(26)^+$ is recovered. When the anion charge is transmitted to one Cl atom *via* π-conjugation at Int5(Na^+), the $Cl(14)^-$ leaving TS, TS5(Na^+), is brought about. A novel trienone intermediate Int6(Na^+) is yielded. The trienone undergoes the nucleophilic addition of HO^- *via* the proton relay (TS6(Na^+)). After the Michael addition, the second substituted phenoxide ion $[C_6H_4(CHClOH)–O^-]$ is recovered at Int7(Na^+). At the same time, the hexagonal pyramidal coordination of $Na(26)^+$ is recovered. From Int7(Na^+), an unprecedented E2 step was found at TS7(Na^+); scission of C(9)–Cl(15) and O(21)–H(10) occurs simultaneously and in the *trans* direction. The novelty is in the proton relay, O(21)→H(10)→O(28)→H(27)→O(2), concomitant with E2. After TS7(Na^+), the product salicylaldehyde is formed.

The H[1,2] migration step reported in ref. 9 was also computed and is shown as TS8(Na^+). TS8(Na^+) was found to cause the change Int3(Na^+)→Int6(Na^+), *i.e.*, trienone.

In the Introduction, the direct *ortho*-formylation was raised, where the C–H bond in the chloroform reactant is retained and becomes a moiety of the aldehyde group in the product. The C–H-retaining reaction is S_N2, exhibited in TS9(Na^+) at the end of Fig. 1. Through the reaction, the phenoxide ion (precursor(Na^+) in Fig. 1) is converted to the dienone intermediate (Int4(Na^+) in Fig. 1).

Except for TS8(Na^+) and TS9(Na^+), seven TSs, *i.e.*, seven elementary processes, were obtained in the present R–T reaction starting from the phenoxide ion.

At TS6(Na^+) in Fig. 1, the nucleophilic addition of the HO^- occurs at the terminal (exocyclic) carbon of the CHCl group of the trienone. The selectivity of the Michael addition is explicable by the shape of the frontier orbital, the LUMO, of the trienone, which is shown in Scheme 6. The largest extension of the LUMO is exactly at the terminal carbon with a coefficient value of 0.56.

Fig. S4 of the ESI† shows the path with K^+ instead of Na^+. Geometric changes of the K^+-containing R–T reaction were found to be similar to those of the Na^+ reaction, except that the trienone in Int6(K^+) is formed directly from the dienone for K^+, Int4(K^+). That is, the dienone→trienone conversion for K^+ is an E2 reaction.

Fig. S5 of the ESI† shows the geometries of three important TSs. The two methods, RB3LYP/6-31(+)G(d) and RB3LYP/6-31+G(d), were found to give similar geometries.

III-3 Energy changes of Na^+- and K^+-containing R–T reactions

Fig. 2 shows the changes of the sum of the B3LYP/6-31+G(d) thermal correction of the Gibbs free energy and the single-point

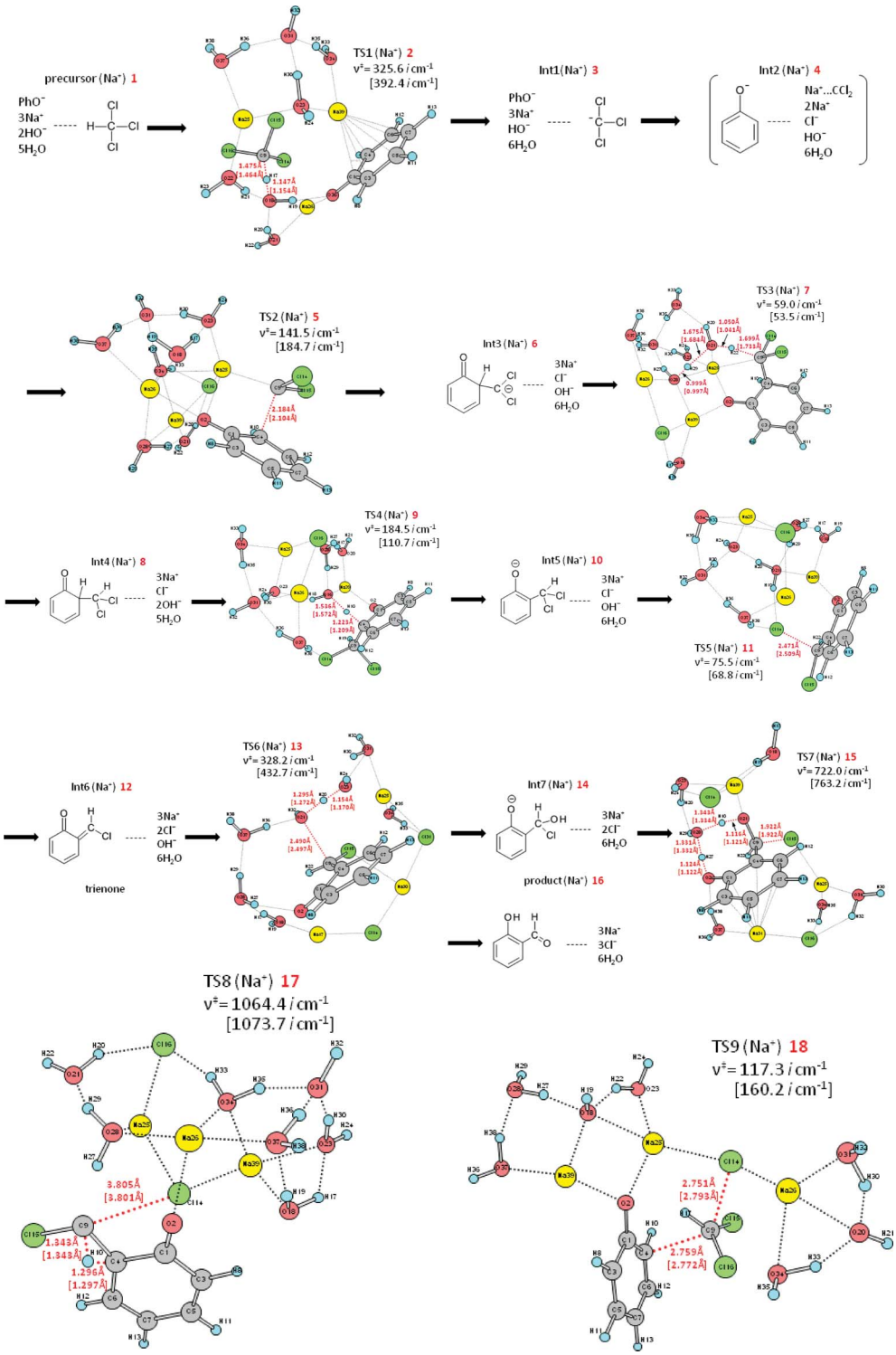

Fig. 1 Geometries of the TSs. Red dotted lines in TSs stand for covalent bonds cleaved or formed. Distances without parentheses are B3LYP/6-3l(+)G(d) and with parentheses are B3LYP/6-31+G(d), respectively. $v^{\ddagger}$ denotes the imaginary frequency to verify that the geometry is at the saddle point. Geometries of the precursor (reactant-like complex, **1**), intermediates (Ints) and the product are shown in Fig. S2 of the ESI.†

B3LYP/6-311+G(d,p) SCRF=PCM electronic energy for the Na^+-containing reaction. These are shown in square brackets in Table S1 of the ESI.† In Table S1, energies without brackets are of B3LYP/6-311+G(d,p) SCRF=PCM // B3LYP/6-31(+)G(d) for both Na^+- and K^+-containing reactions. They are also shown in Fig. S6 of the ESI.† The R–T reaction is shown to be remarkably exothermic with a reaction energy of 110.80 [113.83] kcal mol^{-1}, which is the energy difference between the precursor(Na^+) and the product(Na^+). The reaction also has an extremely high spontaneity, with a sharp energy descent along each elementary process.

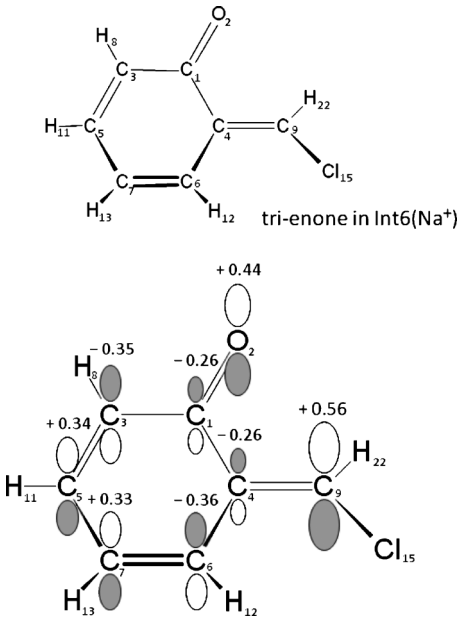

Scheme 6 The shape of the LUMO of the tri-enone intermediate. The lobe on C_9 is the largest (+0.56).

The high reactivity of the R–T reaction was thus revealed. The H[1,2] shift, TS8(Na^+), was calculated to be of high energy (12.34 [12.36] kcal mol^{-1}) and therefore is unlikely. Also, the activation free energy of the S_N2(TS9(Na^+)) reaction was computed to be very large, 29.58 [29.54] kcal mol^{-1}. Thus, the reaction is unlikely because the anionic character of the phenoxide ion is delocalized and the nucleophilicity of the ion is low. Direct *ortho*-formylation is thus ruled out.

The rate-determining step is the electrophilic addition (TS2). While the step is clear with K^+, *i.e.*, $\Delta G^{\ddagger}$(TS2) > $\Delta G^{\ddagger}$(TS1), it is unclear with Na^+, *i.e.*, $\Delta G^{\ddagger}$(TS2) = 11.67 [9.29] kcal mol^{-1} and $\Delta G^{\ddagger}$(TS1) = 9.59 [9.43] kcal mol^{-1}. At TS1(Na^+), proton removal from the chloroform molecule is decelerated by the strong coordination of Na^+ to HO^-. On the contrary, at TS2(Na^+), the strong coordination of Na^+ to CCl_2 enhances its electrophilicity. The strength of Na^+ makes the rate-determining step unclear. This ambiguity was examined by additional calculations of the precursor(Na^+), TS1(Na^+) and TS2(Na^+). The obtained $\Delta G^{\ddagger}$ values are displayed in Table 1. By the six methods, (a–f), TS2(Na^+) is confirmed to be the rate-determining step.

IV. Concluding remarks

In this work, the Reimer–Tiemann (R–T) reaction was investigated by B3LYP calculations. A model composed of $CHCl_3$, $PhO^-(Na^+)H_2O$ and $[NaOH(H_2O)_2]_2$ was employed for geometry optimizations. The K^+-containing model was also investigated. In the Introduction, four questions were raised, and they may be answered in view of the calculated results.

(1) The C–H bond-retaining reaction (*i.e.*, TS9) is unlikely owing to the low nucleophilicity of the *ortho*-carbon of $C_6H_5O^-$.

(2) The dichlorocarbene may intervene in the carbenoid form of Scheme 3. However, it is only transient prior to the electrophilic addition to PhO^-.

(3) Na^+ (or K^+) coordination to CCl_2 enhances its electrophilicity towards $C_6H_5O^-$.

(4) The counter ion Na^+ (or K^+) is indispensable for the R–T reaction. Firstly, it serves in carbenoid formation along with its enhancement. Secondly, the cation stabilizes the precursor phenoxide ion and its substituted intermediates in hexagonal pyramidal coordination. Scheme 7 shows a summary of the present calculations as a revision of Scheme 1.

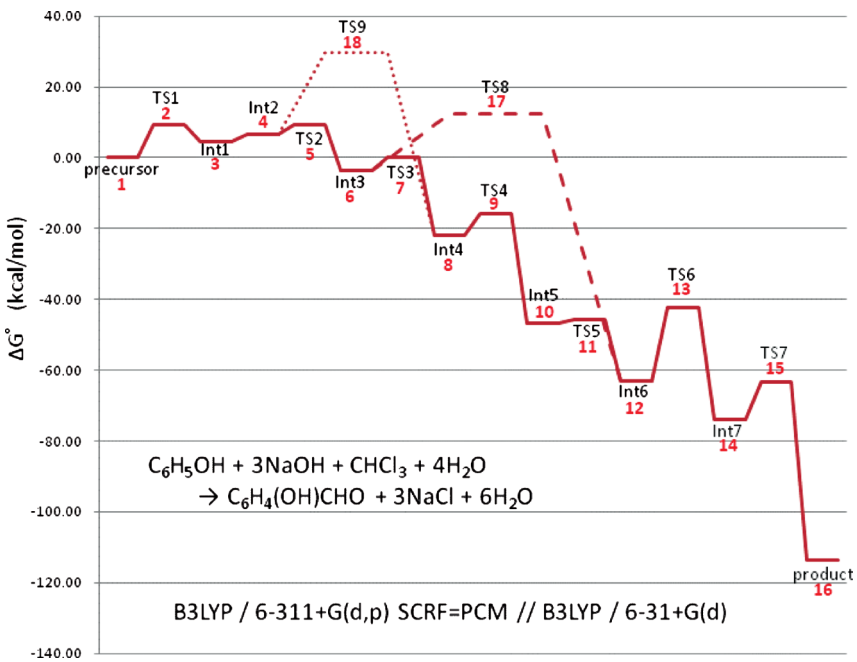

Fig. 2 Energy changes along the paths in Fig. 1. Relative Gibbs free energies of RB3LYP/6-311+G(d,p) SCRF═PCM // RB3LYP/6-31+G(d). RB3LYP/6-311+G(d,p) SCRF═PCM // RB3LYP/6-31(+)G(d) of both Na^+ and K^+ reactions are shown in Table S1 of the ESI.†

Table 1 $\Delta G^{\ddagger}$ values in kcal mol^{-1} (T = 298.15 K, p = 1 atm) calculated by various methods

	Method	TS1(Na$^+$)	TS2(Na$^+$)
	B3LYP / 6-311+G(d,p) SCRF═PCM // B3LYP/6-31(+)G(d) (in Table S1†)	9.594	11.686
	B3LYP / 6-311+G(d,p) SCRF-PCM // B3LYP/ 6-31+G(d) (in Table S1†)	9.428	9.291
(a)	B3LYP / 6-311+G(d,p) SCRF-PCM // B3LYP/6-311+G(d,p)	10.260	12.574
(b)	MPW1K / 6-311+G(d,p) SCRF-PCM // PWlK/6-31(+)G(d)	9.307	16.098
(c)	B3LYP / 6-311++G(2d,p) SCRF-PCM // B3LYP/6-31(+)G(d)	9.854	13.169
(d)	B3LYP / 6-311++G(3df,2p) SCRF-PCM // B3LYP/6-31(+)G(d)	10.536	13.695
(e)	B3PW91 / 6-311++G(3df,2p) SCRF-PCM // B3LYP/6-31(+)G(d)	9.121	15.925
(f)	B3LYP / Aug-CC-pVDZ SCRF═PCM // B3LYP/6-31(+)G(d)	8.902	10.922

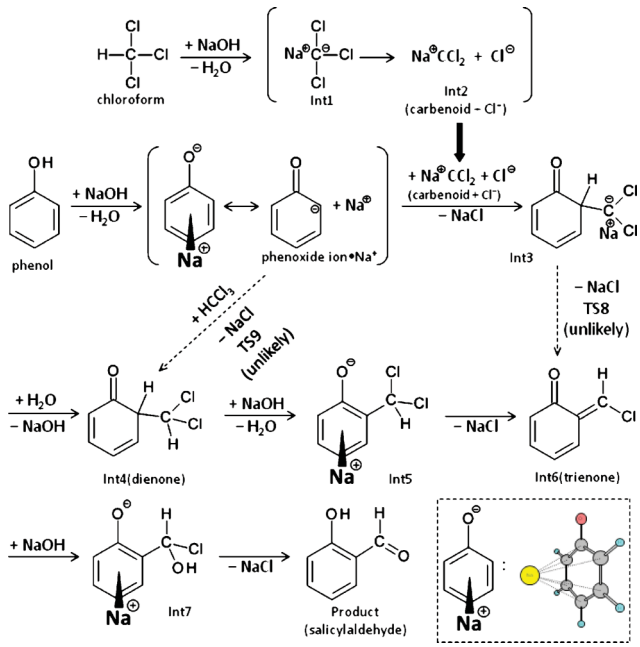

Scheme 7 A summary of the present calculations. Symbols above and below the arrow symbols are the added and eliminated species, respectively. Two dashed arrows, representing direct formylation and H[1,2] shift, indicate unlikely paths. An expression of the Na$^+$ coordination to phenoxide ions is defined in the dashed box. Sums of (+NaOH +NaOH −NaOH +NaOH +NaOH), (−H_2O −H_2O +H_2O −H_2O) and (−NaCl −NaCl −NaCl) correspond to the coefficients in Scheme 1. For K$^+$, intermediate Int5 is absent and the E2 path of Int4 → Int6 is obtained.

The Na$^+$-containing reaction consists of seven elementary processes and the K$^+$-containing reaction of six elementary processes, with extremely high exothermicity and spontaneity. The dienone and trienone are found to be key intermediates in the transformation of the phenoxide derivatives. The electrophilic addition of the carbenoid to PhO$^-$ (*i.e.*, TS2) is the rate-determining step.

References

1 K. Reimer and F. Tiemann, *Ber. Dtsch. Chem. Ges.*, 1876, **9**, 824.
2 M. Srebnik and E. Laloe, Chloroform, *Encyclopedia of Reagents for Organic Synthesis*, John Wiley, New York, 2001. DOI: 10.1002/047084289x.rc105.
3 (*a*) R. M. Dobson and W. P. Webb, *J. Am. Chem. Soc.*, 1951, **73**, 2767; (*b*) O. L. Brady and J. Jakobovits, *J. Chem. Soc.*, 1950, 767; (*c*) D. S. Kemp, *J. Org. Chem.*, 1971, **36**, 202; (*d*) J. C. Cochran and M. G. Melvile, *Synth. Commun.*, 1990, **20**, 609; (*e*) B. R. Langlois, *Tetrahedron Lett.*, 1991, **32**, 3691; (*f*) M. C. Jimenez, M. A. Miranda and R. Tormos, *Tetrahedron*, 1955, **51**, 5825; (*g*) M. E. Jung and T. I. Lazarova, *J. Org. Chem.*, 1997, **62**, 1553.
4 A. Geuther, *Ann.*, 1862, **123**, 121.
5 (*a*) J. Hine, *J. Am. Chem. Soc.*, 1950, **72**, 2438; (*b*) J. Hine, R. C. Peek Jr. and B. D. Oakes, *J. Am. Chem. Soc.*, 1954, **76**, 827; (*c*) J. Hine and A. M. Dowell Jr., *J. Am. Chem. Soc.*, 1954, **76**, 2688.
6 W. von E. Doering and A. K. Hoffmann, *J. Am. Chem. Soc.*, 1954, **76**, 6162.
7 H. Wynberg, *Chem. Rev.*, 1960, **60**, 169.
8 S. Yamabe and N. Tsuchida, *J. Comput. Chem.*, 2004, **25**, 598.
9 R. Castillo, V. Moliner and J. Andres, *Chem. Phys. Lett.*, 2000, **318**, 270.
10 (*a*) A. D. Becke, *J. Chem. Phys.*, 1993, **98**, 5648; (*b*) C. Lee, W. Yang and R. G. Parr, *Phys. Rev. B*, 1988, **37**, 785.
11 T. Clark, J. Chandrasekhar, G. W. Spitznagel and P. v. R. Schleyer, *J. Comput. Chem.*, 1983, **4**, 294.
12 (*a*) K. Fukui, *J. Phys. Chem.*, 1970, **74**, 4161; (*b*) C. Gonzalez and H. B. Schlegel, *J. Chem. Phys.*, 1989, **90**, 2154.
13 (*a*) M. T. Cances, B. Mennucci and J. Tomasi, *J. Chem. Phys.*, 1997, **107**, 3032; (*b*) M. Cossi, V. Barone, B. Mennucci and J. Tomasi, *Chem. Phys. Lett.*, 1998, **286**, 253; (*c*) B. Mennucci and J. Tomasi, *J. Chem. Phys.*, 1997, **106**, 5151.
14 (*a*) Y. Zhao and D. G. Truhlar, *J. Phys. Chem. A*, 2004, **108**, 6908; (*b*) B. J. Lynch, P. L. Fast, M. Harris and D. G. Truhlar, *J. Phys. Chem. A*, 2000, **104**, 4811; (*c*) M. Harańczyk and M. Gutowski, *Internet Electron. J. Mol. Des.*, 2004, **3**, 368.
15 (*a*) J. P. Perdew and Y. Wang, *Phys. Rev. B: Condens. Matter*, 1992, **45**, 13244; (*b*) A. D. Becke, *J. Chem. Phys.*, 1992, **97**, 9173; (*c*) Q. Cui, Z. Liu and K. Morokuma, *J. Chem. Phys.*, 1998, **109**, 56.
16 M. J. Frisch, G. W. Trucks, H. B. Schlegel, G. E. Scuseria, M. A. Robb, J. R. Cheeseman, J. A. Montgomery, Jr., T. Vreven, K. N. Kudin, J. C. Burant, J. M. Millam, S. S. Iyengar, J. Tomasi, V. Barone, B. Mennucci, M. Cossi, G. Scalmani, N. Rega, G. A. Petersson, H. Nakatsuji, M. Hada, M. Ehara, K. Toyota, R. Fukuda, J. Hasegawa, M. Ishida, T. Nakajima, Y. Honda, O. Kitao, H. Nakai, M. Klene, X. Li, J. E. Knox, H. P. Hratchian, J. B. Cross, V. Bakken, C. Adamo, J. Jaramillo, R. Gomperts, R. E. Stratmann, O. Yazyev, A. J. Austin, R. Cammi, C. Pomelli, J. Ochterski, P. Y. Ayala, K. Morokuma, G. A. Voth, P. Salvador, J. J. Dannenberg, V. G. Zakrzewski, S. Dapprich, A. D. Daniels, M. C. Strain, O. Farkas, D. K. Malick, A. D. Rabuck, K. Raghavachari, J. B. Foresman, J. V. Ortiz, Q. Cui, A. G. Baboul, S. Clifford, J. Cioslowski, B. B. Stefanov, G. Liu, A. Liashenko, P. Piskorz, I. Komaromi, R. L. Martin, D. J. Fox, T. Keith, M. A. Al-Laham, C. Y. Peng, A. Nanayakkara, M. Challacombe, P. M. W. Gill, B. G. Johnson, W. Chen, M. W. Wong, C. Gonzalez and J. A. Pople, *GAUSSIAN 03 (Revision E.01)*, Gaussian, Inc., Wallingford, CT, 2004.
17 (*a*) H. E. Simmons and R. D. Smith, *J. Am. Chem. Soc.*, 1958, **80**, 5323; (*b*) E. Nakamura, A. Hirai and M. Nakamura, *J. Am. Chem. Soc.*, 1998, **120**, 5844.

